Projecting of wave height and water level on reef-lined coasts due to intensified tropical cyclones and sea level rise in Palau to 2100

Chuki Hongo[1,2], Haruko Kurihara[1,2], Yimnang Golbuu[3]

[1]Department of Chemistry, Biology, and Marine Science, Faculty of Science, University of the Ryukyus, 1 Senbaru,
Nishihara, Okinawa 903-0213, Japan
[2]JST (Japan Science and Technology Agency)/JICA (Japan International Cooperation Agency)/SATREPS (Science and Technology Research Partnership for Sustainable Development)
[3]Palau International Coral Reef Center, 1 M-Dock Road, PO Box 7086, Koror 96940, Republic of Palau

Correspondence to: Chuki Hongo (g123001@sci.u-ryukyu.ac.jp)

Abstract. Tropical cyclones (TCs) and sea level rise (SLR) cause major problems including beach erosion, saltwater intrusion into groundwater, and damage to infrastructure in coastal areas. The magnitude and extent of damage is predicted to increase as a consequence of future climate change and local factors. Upward reef growth has attracted attention for its role as a natural breakwater, reducing the risks of natural disasters to coastal communities. However, projections of change in the risk to coastal reefs under conditions of intensified TCs and SLR are poorly quantified. In this study we projected the wave height and water level on Melekeok reef in the Palau Islands by 2100, based on wave simulations under intensified TCs (significant wave height at the outer ocean: SWH_o = 8.7–11.0 m; significant wave period at the outer ocean: SWP_o = 13–15 s) and SLR (0.24–0.98 m). To understand effects of upward reef growth on the reduction of the wave height and water level, the simulation was conducted for two reef condition scenarios: a degraded reef and a healthy reef. Moreover, analyses of reef growth based on a drilled core provided an assessment of the coral community and rate of reef production necessary to reduce the risk from TCs and SLR on the coastal areas. According to our calculations under intensified TCs and SLR by 2100, significant wave heights at the reef flat (SWH_r) will increase from 1.05–1.24 m at present to 2.14 m if reefs are degraded. Similarly, by 2100 the water level at the shoreline (WL_s) will increase from 0.86–2.10 m at present to 1.19–3.45 m if reefs are degraded. These predicted changes will probably cause beach erosion, saltwater intrusion into groundwater, and damage to infrastructure, because the coastal village is located at ~3 m above the present mean sea level. These findings imply that even if the SWH_r is decreased by only 0.1 m by upward reef growth, it will probably reduce the risks of costal damages. Our results showed that a healthy reef will reduce a maximum of 0.44 m of the SWH_r. According to analysis of drilled core, corymbose *Acropora* corals will be key to reducing the risks, and 2.6–5.8 kg $CaCO_3/m^2/y$, equivalent to >8% of coral cover, will be required to keep a healthy reef by 2100. This study highlights that the maintaining reef growth (as a function of coral cover) in the future is effective in reducing the risk of coastal damage arising from wave action. Although the present study focuses on Melekeok fringing reef, many coral reefs are in the same situation under conditions of

intensified TC and SLR, therefore the results of this study are applicable to other reefs. These researches are critical in guiding policy development directed at disaster prevention for small island nations, and for developing and developed countries.

1 Introduction

5   Approximately 90 tropical cyclones (TCs; also referred to as hurricanes and typhoons) occur globally every year (Frank and Young, 2007; Seneviratne et al., 2012). TCs cause large waves, storm surges, and torrential rainfall, and can lead to coastal erosion, salinization of coastal soils, and damage to infrastructure (Gourlay, 2011a). These negative impacts have major economic loss. For example, the economic cost of TC Pam (category 5 on the Saffir–Simpson scale), which affected Vanuatu in March 2015, exceeded US$449 million, equivalent to ~64% of the GDP of Vanuatu (GFDRR, 2016).

10   Numerical projections indicate that climate change will increase the mean maximum wind speed of TCs (Christensen et al., 2013). Towards the end of the 21st century, the wind speed and minimum central pressure of the most intense super typhoons in the northwest Pacific Ocean are estimated to attain 85–90 m/s and 860 hPa, respectively (Tsuboki et al., 2015). This will probably increase wave heights and water levels on shores at coastal areas. Additionally, sea level rise (SLR) caused by global warming will probably increase the risk of coastal erosion, flooding, and saltwater intrusion of

15   surface water (Woodruff et al., 2013). Economic development and population growth are also expected to increase along the coastal areas, increasing the potential cost of damages to coastal community's baseline damages (World Bank and UN, 2010). Therefore, the development of policies for adaptation to TCs and SLR is essential if their projected negative impacts in the near future are to be adequately addressed.

Several approaches to reduce the wave heights and water levels have been suggested, including the construction of

20   sea walls and shelters, developing accurate weather forecasts, and developing TC and SLR warning systems (GFDRR, 2016). However, small island nations and developing countries will need to develop cost-effective strategies to address the problems associated with these phenomena, including the use of ecosystem services provided by mangroves and coral reefs. For example, mangrove restoration has been demonstrated to attenuate wave height, and reduce wave damage and erosion (Wong et al., 2014). More than 150,000 km of the shoreline in 100 countries and territories receive some protection from

25   reefs (Burke et al., 2011). Meta analysis has demonstrated that the entire reef system, from reef slope to reef flat, reduces wave height by an average of 84% (Ferrario et al., 2014). Coral reefs are also habitats for diverse marine organisms and provide various services (e.g., tourism and marine products) that benefit human populations. Additionally, reefs can be considered to represent self-adapting "green infrastructure" (Benedict and McMahon, 2002) in the ocean that protects against TCs and SLR. The growth of Holocene reefs has kept pace with the SLR that occurred in the period 19–6 ka (Montaggioni

30   and Braithwaite, 2009). This suggests that reef growth, as a form of green infrastructure, may be able to respond to SLR and contribute to the reduction of the wave heights and water levels at shores in the future.

However, approximately 75% of the world's coral reefs are subject to local threats such as coastal development, watershed pollution, and overfishing (Burke et al., 2011). Additionally, global climate change, including global warming and ocean acidification, is expected to have major impacts on coral reefs. For example, corals around the world died in large numbers; as much as 95 % mortality was seen in many parts of the Indian Ocean, including the Seychelles (Sheppard et al., 2005). The coral mortality led to a decrease in reef bottom roughness, which resulted in the ability of the reef to dissipate wave energy across the reefs in Seychelles from 1994 to 2004 (Sheppard et al., 2005). Ocean acidification reduces the $CaCO_3$ saturation rate and coral growth, reducing the calcification of corals (Anthony et al., 2008). This process also reduces the roughness of reef flats and consequently higher wave energy reaches the shore. This indicates that the degraded reef may cause an increase in wave heights and water levels at shores in the future. However, there is still almost no quantitative study evaluating the effectiveness of reefs to TCs and SLR on degraded versus healthy reefs. Furthermore, if future reefs are degraded, considering potential supplementations (e.g., by coral transplantation) will be needed. The target corals for the transplantation are also poorly understood.

This study focuses on coral reefs in Palau Islands. The Palau Islands are rarely affected by TCs, but two severe TCs (Typhoon Bopha in 2012 and Typhoon Haiyan in 2013) recently impacted the islands. These TCs caused 56%−83% loss of coral cover on the shallow slopes of the eastern reefs (Gouezo et al., 2015), and they had a significant impact on coastal areas (e.g., flooding, erosion, and destruction of buildings). Additionally, intensity of TCs is expected to increase under future conditions in the northwest Pacific (Tsuboki et al., 2015). Furthermore, there will probably be an eastward shift in the genesis location of TCs in the northwest Pacific in the near future (2075–2099; Murakami et al., 2011). This implies that Palau Islands, which currently experience only infrequent and lower intensity TCs, will probably be affected by more frequent and intense TCs in the near future. Consequently, this study has two main aims. Firstly, we provide a quantitative projection of wave heights and water levels for the healthy reefs and the degraded reefs under intensified TCs and SLR conditions by 2100, based on a numerical simulation. Secondly, we estimate the potential of main reef builder and the reef production rate necessary to reduce the coastal risk under the predicted reef degradation, based on analysis of a drilled core that looked at past reef growth and carbonate production.

2 Methods

2.1 Study site

The present study site is located in Melekeok state, at the east central coast of Babeldaob, the biggest island in Palau (Figure 1a). Melekeok reef (7.501°N, 134.640°E) is located on the eastern coast of the state. Melekeok is an important state because it is the national capital of Palau, housing the national government including the executive, legislative and judiciary branch of the government. Melekeok is an ideal site for this study because it is representative of the east coast of Palau in terms of its closeness to the sea and risk of negative impacts from waves and sea level rise. Understanding the situation in Melekeok

can be applied to other states on the east coast of Palau in terms of preparedness for the future impacts of climate change. The state consists of reefs, long beaches, mangroves, hills, steep ridges, and rivers. Prior to the contact with foreigners, some of the villages started to increase their influence and power by forming alliances through warfare (Rechebei and McPhetres, 1997), and Melekeok and Koror village became the most powerful villages in the islands. During the Japanese administration (1919–1945), the settlement of the state had moved to the coastal area from inland. In the present-day, the coastal village is located at ~3 m above the present mean sea level (MSL). The Melekeok Elementary School and Melekeok State Office are also located along the coast. There is no artificial breakwater for ocean waves along the reef. Our survey transect is located near the elementary school (Figure 1b), because the school will probably be a place to evacuate during assumed intensified TCs.

2.2 Impacts of historical TCs and Typhoon Bopha

Since 1951, 19 TCs passed within 150 km of Melekeok reef in Palau, provided by the Digital Typhoon (http://agora.ex.nii.ac.jp/digital-typhoon/index.html.en) based on the Japan Meteorological Agency (JMA) best track data (Table 1). Only one severe TC passed near this study reef in 1990 (Typhoon Mike), and the impact was limited to the northern reef of Palau (Maragos and Cook, 1995). Prior to Typhoon Bopha, which passed south of Palau on 2 December 2012, it is suspected that no major TCs had caused significant damage to coral reefs and coastal areas of Palau for over 60 years.

The minimum pressure of Typhoon Bopha center was 935 hPa and the maximum wind speed was 50 m/s (data obtained by Digital Typhoon: http://agora.ex.nii.ac.jp/digital-typhoon/index.html.en). On 2 December 2012, the average wind speed was 27 m/s around the study site, simulated by using the Global Forecast System (GFS) model at 27 km resolution, provided by Windguru (see http://www.windguru.cz), 121 km distance from the track of Typhoon Bopha (Figure 1a). On 6–7 November 2013, Typhoon Haiyan passed north of Palau Islands. The minimum pressure of Typhoon Haiyan center was 905–920 hPa (data obtained by Digital Typhoon: http://agora.ex.nii.ac.jp/digital-typhoon/index.html.en) (Figure 1a). In the Northern Hemisphere, TCs rotate in a counterclockwise direction and the most severe conditions are generated in the right semicircle, where the maximum wind speeds and storm surge are localized. Therefore, the average wind speed of Typhoons Bopha was stronger than that of Haiyan around the study site. Similarly, the maximum value of significant wave height at offshore in the study site was 8.7 m on 2 December 2012 during Typhoon Bopha and was 7.7 m on 7 November 2013 during Typhoon Haiyan, by the simulation using GFS model at 27 km resolution (obtained from Windguru; see http://www.windguru.cz). Consequently, the study site was severely damaged (e.g., the destruction of piers and flooding) by Typhoon Bopha.

2.3 Estimation of wave height and water level

We focused on two parameters: (1) the significant wave height (SWH) at the reef flat (SWH_r), located 400 m from the shore; and (2) the averaged water level at the shore (WL_s). SWH was defined as the mean wave height of the highest 33% of waves. We attempted to find *in situ* recorded data of ocean wave and water level using underwater loggers and/or radar observational systems at the study site, but there was no *in situ* observation data for ocean wave and water level at the study site. Therefore, we conducted an estimation of wave height and water level based on the CADMAS-SURF (Super Roller Flume for Computer Aided Design of Marine Structure) wave simulation model (CDIT, 2001). For validation of the model, we compared calculated results with *in situ* measurements of SWH and WL at the reef flat, which is located 400 m from the shore, under non-TCs conditions. Moreover, we conducted local interviews to obtain reliable information of the impacts of Typhoon Bopha.

The CADMAS-SURF model is a specialized numerical wave tank model used for assessing the threshold of destruction for structures (e.g., sea walls) and it contributes to coastal management decisions. The governing equation in the model is based on the extended Navier–Stokes equations for a two-dimensional wave field in porous media. The model can reproduce highly non-linear wave profiles against various structures (e.g., impact of a wave breaking sea walls) (Isobe et al., 1999). The model can express wave deformations (e.g., wave shoaling, wave breaking, wave overtopping, and wave run-up) at coral reefs. Nagai and Shiraishi (2004) and Kawasaki et al. (2007; 2008) validated the model by comparing the results obtained by the CADMAS-SURF model with observed data and laboratory experiments on wave deformation over coral reefs under TC conditions, therefore the model has been successfully applied to wave characteristics at coral reefs under TC conditions (Yamashita et al. 2008; Hongo et al. 2012; Nakamura et al. 2014; Watanabe et al. 2016).

To calculate wave characteristics in the model, we input the following parameters: (1) wave condition; (2) obstacle data (e.g., reef structure and road); (3) time control; (4) mesh size; and (5) physical parameter (e.g., density of water). Details of the parameters are shown in CDIT (2001). To determine a wave condition, we need to input three parameters: incident significant wave height at the outer ocean (SWH_o); incident significant wave period at the outer ocean (SWP_o); and incident water level at the outer ocean (WL_o). The parameters are discussed below.

SWH_o: Since there is no *in situ* observation system for ocean wave and water level at offshore and onshore in Palau Islands, the present-day SWH_o value was simulated by using the GFS model at 27 km resolution, provided by Windguru (see http://www.windguru.cz). The values for 4 sites (Melekeok, Koror, North beaches, and West Passage) are provided by the GFS model. The GFS model provided a regular wave. In this study, we input the regular wave as a forcing into the CADMAS-SURF model. The largest SWH_o value at Melekeok during Typhoon Bopha was simulated to be 8.70 m. Numerical experiments have shown that the maximum wind speeds of TCs in the northwest Pacific will increase by 19% by the late 21st century as a consequence of global warming (Tsuboki et al., 2015). This implies that SWH_o will increase in the future, but will probably vary among study sites as a function of wind speed and the path of TCs. Projecting wind speed

depends on future greenhouse gas emissions. Therefore, we assumed that TCs are characterized by a minimum central pressure of ca. 900 hPa. We also assumed that the future maximum SWH_o at Palau reef will be comparable to the TCs that typically affect the Ryukyu Islands (northwest Pacific). These include Typhoons Shanshan in 2006 and Talim in 2005, which JMA reported had wind speeds and SWH_o of 26–34 m/s and 10.6–11.3 m, respectively (JMA, 2012; see

5   http://www.data.jma.go.jp/gmd/kaiyou/db/wave/chart/daily/coastwave.html). Consequently, we assumed that by 2100 the SWH_o will range from 8.70 to 11.0 m.

SWP_o: The SWP_o was simulated by using the GFS model, which was calculated to be 13.0s during Typhoon Bopha peak period (P_{peak}). The empirical P_{peak}:SWP ratio is approximately 1 (≈ 0.95); consequently, we assumed the value of P_{peak} equated to SWP_o. As an analogy, the SWP_o during the severe typhoons Shanshan and Talim in the Ryukyu Islands was 13.0–

10   15.0 s (see JMA: http://www.data.jma.go.jp/gmd/kaiyou/db/wave/chart/daily/coastwave.html). Therefore, we assumed that the future SWP_o at Palau reef will range from 13.0 to 15.0 s. We input the SWP_o as a regular wave into the model.

WL_o: We assumed that the WL_o ranges from 0 to 2.78 m above the present MSL, based on future SLR, tidal ranges, and storm surges. The future SLR is predicted to range from +0.24 m to +0.30 m by 2050, and from +0.44 m to +0.98 m by 2100, based on the Intergovernmental Panel on Climate Change (IPCC) scenarios Representative Concentration Pathway

15   (RCP) 2.6 and RCP 8.5, respectively (Church et al., 2013). The RCP was used for the new climate model simulations carried out under the framework of the Coupled Model Intercomparison Project Phase 5 of the World Climate Research Programme. For RCP 2.6, the radiative forcing peaks at approximately 3 W/m^2 before 2100 and then declines (IPCC, 2013). For RCP 8.5, the radiative forcing reaches greater than 8.5 W/m^2 by 2100 and continues to rise for some amount of time (IPCC, 2013). At Palau Islands, the tidal range is ~1.60 m during spring tides, and the high tide is ~0.80 m above MSL. Storm surges lead to

20   extreme SLR when TCs make landfall. We assume that intensified TC is characterized by a minimum central pressure of ca. 900 hPa, and thus WL_o will increase to 1.00 m above MSL as a result of the suction effect of TC.

In the model, we input a topographic profile. To determine the topography, we established a transect of 2000 m width that extended from 21 m above MSL at the shore to 269 m water depth in the outer ocean (Figure 1b). The topography along the transect was determined using a topographic map (USGS, 1983) on land, and was measured using an automatic

25   level (NIKON-TRIMBLE, AE-7) and an aluminum staff from the shore to the reef crest, and a single beam echo sounder (Honda Electronics, PS-7) on the reef slope at water depths of 0–75 m. At water depths of 75–269 m the topography was assumed to increase with depth at an angle of 23°. The field survey was conducted in July and September 2015. In this study, we used two reef condition scenarios. The first was that reefs are healthy and have a growth rate equal to the SLR from the reef crest to the upper reef slope, and the second was that the reef is degraded and no growth occurs (Figure 1c). The

30   difference between healthy reefs and degraded reefs was expressed as the topographic profile in the model.

In this model, the time step was 0.01 s and the calculation time was 3600 s. We used outputs in the time interval for 1801–3600 s. The horizontal mesh size was set as $\Delta x = 20$ m. The vertical mesh size was $\Delta y = 1$–5 m. We used fine vertical mesh sizes for the land to the reef edge and coarse ones for the outer ocean. The density of water was set as 1025 kg/m^3. The

porosity of the reef structure is 10 %. In this model, we could not input the reef bottom roughness. The input parameters (e.g., WL_o) are given to two decimal places because the future SLR is given to two decimal places (e.g., +0.24 m: Church et al., 2013). Therefore, the calculated values of SWH_r and WL_s are given to two decimal places. The data for SWH_r were calculated using the output from the zero-up crossing method.

5   We performed a sensitivity analysis to clarify the change of SWH_r and WL_s in response to intensity of TCs at various SLR and storm surge scenarios (Tables S1 and S2). Additionally, we investigated the effects of SLR at various TC and storm surge conditions and the effects of storm surge at various TC and SLR conditions.

2.4 *In situ* measurement and calculation for model validation

For validation of the CADMAS-SURF model, we measured WL and SWH at the study site despite non-TC conditions. We
10   deployed one water level logger (Onset HOBO) on the reef flat, which is located 400 m from the shore, from 31 October to 1 November 2017. The logger sampled every 1 s. The logger was corrected for atmospheric pressure variations using another water level logger (Onset HOBO) deployed on land. We used three sets of 30-min measured data. The sampling details are summarized in Table 2.

        We conducted a calculation of WL and SWH on the reef flat, which is located 400 m from the shore, based on the
15   CADMAS-SURF model. We assumed that the SWH_o ranges from 1.20 to 1.30 m, the SWP_o ranges from 12.0 to 14.0 s, and the WL_o ranges from 0.50 to 0.90 m above the present MSL, from 31 October to 1 November 2017. The data of SWH_o and SWP_o were obtained from Windguru (see http://www.windguru.cz). The details of input parameters are summarized in Table 2.

2.5 Estimation of future reef production rate

20   We estimated the potential future rate of reef production (kg $CaCO_3/m^2/y$) using a drilled core from the reef crest at Ngerdiluches reef in the Palau Islands (Figure 1a). One reef crest core (PL-I; 25 m long) was recovered from Ngerdiluches reef (Kayanne et al., 2002). The thickness of the Holocene sequence is 14.5 m long. The Holocene sequence comprised two facies: (1) corymbose *Acropora* facies; and (2) arborescent *Acropora* facies (Hongo and Kayanne, 2011). The corymbose *Acropora* facies is characterized by corymbose and tabular *Acropora* (e.g., *Acropora digitifera*). These corals are found on
25   distinct reef crests and upper reef slopes in Palau Islands (Kayanne et al., 2002; Yukihira et al., 2007). The zone is generally characterized by high-energy waves in water depths less than 7 m (Hongo and Kayanne, 2011). The arborescent *Acropora* facies is dominated by *Acropora muricata/ intermedia* complex. These corals occupy the inner reef slope and leeward reef slope at water depths of less than 20 m in Palau Islands and other reefs in the present-day Pacific Ocean (Montaggioni, 2005; Yukihira et al., 2007). These corals are presented at places with low- to moderate- energy wave conditions (Hongo and
30   Kayanne, 2011).

We weighed all samples and measured the density of each facies. Assuming that the reef crest has a homogenous structure, the production rate of the reef crest is given by:

$$R = \frac{\rho H}{t} \qquad (1)$$

where R (kg CaCO$_3$/m^2/y) is the production rate of the reef crest, ρ is the density (kg CaCO$_3$/m^3), H (m) is the thickness of the reef crest, and t (y) is the duration of vertical reef formation. We used two reported radiocarbon ages for arborescent *Acropora* facies (PL- I-79: 8.31 ka, −15.1 m below MSL; PL- I-67: 7.39 ka, −12.0 m below MSL) and four radiocarbon ages for corymbose *Acropora* facies (PL- I-43: 7.25 ka, −6.8 m below MSL; PL- I-26: 7.15 ka, −4.4 m below MSL; PL- I-8: 6.28 ka, −2.5 m below MSL; PL- I-3: 3.92 ka, −1.8 m below MSL) (Kayanne et al., 2002; Hongo and Kayanne, 2011). We assumed that the range of upward reef growth rate (i.e., *H/t*) was 3.4–37.1 m/kyr (between samples PL- I-79 and PL- I-67, and samples PL- I-67 and PL- I-43) for arborescent *Acropora* facies in response to 10 m/kyr of Holocene SLR. Similarly, we assumed that the upward reef growth rates for the corymbose *Acropora* facies in response to 10 m/kyr, 5 m/kyr, and <5 m/kyr of Holocene SLR were 24.0 m/kyr (between samples PL- I-43 and PL- I-26), 2.2 m/kyr (between samples PL- I-26 and PL- I-8), and 0.3 m/kyr (between samples PL- I-8 and PL- I-3), respectively.

3 Results

3.1 Model validation

Figure 2 shows maximum and minimum values of calculated WL and measured WL on the reef flat at the study site. The mean of calculated WL and measured WL were 0.96 and 0.87 m (Test 1), 0.64 and 0.54 m (Test 2), and 0.56 and 0.54 m (Test 3), respectively. The calculated mean WL on the reef flat slightly exceeded (0.07 m) the measured mean values. Similarly, measured SWH and calculated SWH were 0.11 and 0.18 m (Test 1), 0.26 and 0.11 m (Test 2), and 0.22 and 0.10 m (Test 3), respectively. The difference in mean value of SWH between measurements and calculations was found to be 0.07 m. The results showed good correspondence between measurements and calculation data. Therefore, we adopted the calculation results for this study.

3.2 Wave height and water level at Typhoon Bopha

Melekeok reef has distinctly zoned landforms, comprising the reef flat and reef slope (Figure 1c). The reef flat is ~1000 m wide and consists of a shallow lagoon (900 m wide) and a reef crest (100 m wide). The shallow lagoon (~1 m deep) is situated between the shore and the reef crest. During the Typhoon Bopha, local people mentioned that beach erosion and destruction of structure (e.g., the pier and a pavilion, ~3 m above MSL) occurred along the shore at the study site (Figure 3). Moreover, the road and the ground of elementary school (+2.86 m above MSL) along the shore were flooded and that this was never seen for the past ca. 70 years.

According to our wave simulation, the SWH_o was found to rapidly decrease from the upper reef slope to the reef crest (Figure 4). Tables 3 and 4 showed all calculated results for SWH_r and WL_s. Cases 1, 15, 30, and 44 presented the results calculated at present condition for Typhoon Bopha, while the other cases presented the results calculated at future conditions by 2100 (sections 3.3 and 3.4). Under present-day TCs (8.70 m SWH_o, 13.0 s SWP_o), the SWH at the reef crest was 2.15 m and the SWH_r was 1.05 m (case 1, Table 3). The reef crest dissipated 75.3% of the SWH_o. The shallow lagoon dissipated 51% of the remaining wave height at the reef crest. The entire reef dissipated 87.9% of the SWH_o. Moreover, the SWH_r was 1.24 m for storm surge under the present-day TCs (case 15, Table 3) and the entire reef dissipated 85.7% of the SWH_o.

The WL_s was 0.86 m for present-day TCs (case 30, Table 4) and the WL_s increased to 2.10 m under storm surge conditions (case 44, Table 4). Moreover, the water level at the shore under present-day TCs (i.e., Typhoon Bopha) reached the elevation of road (+2.86 m above MSL) at the study site (Figure 5).

3.3 Future wave height at the reef flat

The SWH_r was found to increase to a maximum of 2.14 m for degraded reefs and to 1.80 m for healthy reefs under intensified TCs, SLR, and storm surges by 2100 (Table 3). An increase in the intensity of TCs will cause an increase in the SWH_r. For example, a SWH_r value of 1.22 m for a healthy reef under present TC conditions (8.70 m SWH_o, 13.0 s SWP_o) (case 16) will increase to 1.52 m (+24.6%) in 2050 with more intense TCs (10.0 m SWH_o, 14.0 s SWP_o) (case 18), and increase to 1.66 m (+36.1%) with the most intense TCs (11.0 m SWH_o, 15.0 s SWP_o) (case 20). Overall, the increase in TC intensity will increase the SWH_r by 38.0 ± 16.0% (mean ± SD, n = 17) for degraded reefs and by 30.7 ± 18.2% (mean ± SD, n = 17) for healthy reefs (Table S1).

Moreover, the SLR will cause a slight increase in the SWH_r. For example, 1.66 m in SWH_r at a healthy reef under the most intense TCs (11.0 m SWH_o, 15.0 s SWP_o) and 0.24 m in SLR (case 20) will increase by 0.30 m in SLR to 1.70 m (+2.4%, 0.30 m in SLR; case 21) and to 1.77 m (+6.6%, 0.44 m in SLR; case 27). Consequently, the effect of SLR will increase the SWH_r by 6.5 ± 11.0% (mean ± SD, 21) at degraded reefs and by 3.0 ± 9.2% (mean ± SD, n = 23) at healthy reefs (Table S1).

Furthermore, storm surges (1.00 m) will also increase the SWH_r. For example, storm surges will cause an increase in the SWH_r from 1.09 m to 1.35 m (+23.9%) at healthy reefs subject to a TC (8.70 m SWH_o, 13.0 s SWP_o; between cases 3 and 17). As another example, under the most intense TCs (11.0 m SWH_o, 15.0 s SWP_o; between cases 6 and 20), storm surges will cause an increase in the SWH_r at healthy reefs from 1.49 m to 1.66 m (+11.4%). Consequently, storm surges will increase the SWH_r by 20.1 ± 14.9% (mean ± SD, n = 13) at degraded reefs, and by 17.3 ± 14.8% (mean ± SD, n = 14) at healthy reefs (Table S1).

The modeling showed that in all but 6 cases (cases 3, 6, 14, 17, 23, and 26) the SWH_r was reduced by 0.01–0.44 m by upward reef growth by 2100 (Table 3, Figure 6). For example, 0.24 m in upward reef growth caused a 0.24 m reduction in

the SWH_r (from 1.45 m for degraded reef to 1.21 m for healthy reef) under more intense TCs (10.0 m SWH_o, 14.0 s SWP_o) (case 4). This indicates that reef growth enhanced the reduction in wave height from 85.5% at degraded reefs to 87.9% at healthy reef (case 4, Table S1). Similarly, under the most intense TCs (11.0 m SWH_o, 15.0 s SWP_o), SLR (0.98 m), and storm surge (1.00 m) in 2100 (case 29), 0.98 m in reef growth caused a 0.20 m reduction in the SWH_r (from 2.00 m for the

5   degraded reef to 1.80 m for the healthy reef); thus, the role of the reef as a natural breakwater increased from 81.8% for the degraded reef to 83.6% for the healthy reef (Table S1). Overall, as a result of reef growth, the wave reduction rate increased from 84.6% at degraded reefs to 86.0% at healthy reefs (Table S1).

3.4 Future water level at the shore

The modeling showed that the WL_s will increase from 0.86–2.10 m at present to 1.19–3.45 m at degraded reefs and to 1.24–

10   3.51 m at healthy reefs under intensified TCs, SLR, and storm surges by 2100 (Table 4, Figure 7). An increase in the intensity of TCs will cause an increase in the WL_s. For example, a 1.24 m WL_s at a healthy reef under a present modeled TC (8.70 m SWH_o, 13.0 s SWP_o) (case 31) will increase to 1.55 m (+25.0%) under more intense TCs (10.0 m SWH_o, 14.0 s SWP_o) (case 33), and increase to 1.90 m (+53.2%) under the most intense TCs (11.0 m SWH_o, 15.0 s SWP_o) by 2050 (case 35). Overall, the increase in intensity of TCs resulted in the increase of WL_s by 22.7 ± 15.3% (mean ± SD, n = 17) for the

15   degraded reef and by 21.4 ± 13.3% (mean ± SD, n = 17) for the healthy reef (Table S2).

The WL_s will also be increased by SLR. For example, the WL_s at a degraded reef subjected to a present modeled TC (8.70 m SWH_o, 13.0 s SWP_o) increased from 1.19 m with 0.24 m SLR (case 31) to 1.50 m (+26.1%) with 0.44 m SLR (case 37), and to 1.82 m (+52.9%) with 0.74 m SLR (case 38). Overall, SLR increased the WL_s by 8.7 ± 18.1% (mean ± SD, n = 21) for the degraded reef and by 32.2 ± 37.8% (mean ± SD, n = 23) for the healthy reef (Table S2).

20   Storm surge also directly increased WL_s. For example, by 2050 this effect caused an increase in WL_s from 1.87 m to 2.87 m (+1.00 m, +53.5%) for the degraded reef and from 1.90 m to 2.86 m (+0.96 m, +50.5%) for the healthy reef under the most intense TCs (11.0 m SWH_o, 15.0 s SWP_o) and SLR (0.24 m) (cases 35 and 49, Table S2). Overall, storm surge significantly increased the SWH_r by 56.5 ± 17.2% (mean ± SD, n = 13) for the degraded reef and by 59.5 ± 27.7% (mean ± SD, n = 14) for the healthy reef (Table S2).

25   The difference in WL_s between degraded and healthy reefs was found to range from only –0.11 to 0.07 m by 2100. For example, by 2050 no difference in WL_s was found between the degraded and healthy reefs under intense TCs (11.0 m SWH_o, 15.0 s SWP_o) and SLR of 0.30 m (case 50). Similarly, a difference of only 0.01 m in WL_s was found between degraded and healthy reefs under more intense TCs (10.0 m SWH_o, 14.0 s SWP_o) (case 55), even with a difference of 0.74 m in upward reef growth.

30   We found that the road (+2.86 m above MSL) adjacent to the study site will be flooded in both degraded and healthy reefs scenarios in 7 cases (cases 49, 50, 53, 55, 56, 57, and 58, Table 4) under conditions of intensified TCs, SLR, and storm surge. In the worst scenario, under the most intense TCs (11.0 m SWH_o, 15.0 s SWP_o), 0.98 m SLR, and a storm

surge of 1.00 m, the WL_s was found to increase to 3.45 m for the degraded reef and to 3.51 m for the healthy reef by 2100 (case 58).

3.5 Potential reef production in mitigating wave risk

The Holocene reef density (ρ), determined from the PL-I core, was 720 kg $CaCO_3/m^3$ for arborescent *Acropora* facies and
5   590 kg $CaCO_3/m^3$ for corymbose *Acropora* facies. The estimated reef production rate (R) ranged from 2.4 to 26.7 kg $CaCO_3/m^2/y$ for arborescent *Acropora* facies, and from 0.3 to 14.2 kg $CaCO_3/m^2/y$ for corymbose *Acropora* facies, depending on the upward reef growth rate and the Holocene SLR (Figure 8). The lower part of the reef was composed of both arborescent and corymbose *Acropora* facies when SLR was 10 m/kyr, whereas the upper part of the reef comprised only corymbose *Acropora* facies when SRL was <5 m/kyr.

10   The value of R needed for Melekeok reef keep pace with SLR by 2100 was calculated to be 5.3 to 7.1 and 2.6 to 5.8 kg $CaCO_3/m^2/y$ for arborescent *Acropora* and corymbose *Acropora* facies, respectively, based on the assumption that the future $CaCO_3$ density and reef growth rate will be equivalent to those of the Holocene reef (Figure 8).

4 Discussion

4.1 Wave height and water level increase in the future

15   Our results show that present-day Melekeok reef is highly effective in dissipating waves, with the reef crest alone reducing the SWH_o by 75% and the entire reef able to reduce the wave height by 88%. Other reefs (e.g., US Virgin Island, Hawaii, Australia, and Guam) have been reported to reduce wave height by an average 64% (n = 10, 51%–71%) at the reef crest, and by an average of 84% (n = 13, 76%–89%) for the entire reef (Ferrario et al., 2014). Generally, greater wave dissipation efficiency is associated with steep topography from the upper reef slope to the reef crest, because of the rapid decrease in
20   water depth (i.e., shoaling of waves), and wider reef flats are reported to have greater dissipation efficiency (Sheppard et al., 2005). The reef in the present study is characterized by a steep reef topography and a wide reef flat (~1000 m wide).

       Our wave calculations showed that increasing TC intensity, SLR, and storm surges will cause an increase in SWH_r by 2100. During future TCs, an increasing wind speed will directly cause increasing SWH_o. Water tank experiments showed a positive relationship between SLR and increasing wave height (Takayama et al., 1977). Sheppard et al. (2005) reported a
25   positive relationship between SLR and wave energy density (an increase in SLR of ~0.2 m increased the density by ~100 J/m^2) at the Seychelles, with the density being proportional to the wave height squared.

       Based on the water level calculated from our model, the road along the shore at this study site will be flooded when simulated with present TC conditions (i.e., Typhoon Bopha). Our simulation was confirmed by the observation of the local people during Typhoon Bopha. The present results also show that increasing TC intensity, SLR, and storm surges will
30   cause an increase in WL_s of Melekeok reef by 2100, with SLR and storm surges directly increasing the WL_s. Furthermore,

an increase in SWH_o as a result of the increasing intensity of TCs will cause an increase in WL_s. An increase in WL_s is likely to be explained by the wave set-up. Wave set-up occurs if waves break in the reef crest–reef slope zone; the wave thrust decreases as the breaking surge travels shoreward, and consequently the water level rises (Gourlay, 2011b). Laboratory experiments and field observations have generally indicated that wave set-up increases with increasing incident wave height and wave period (Nakaza et al., 1994; Gourlay, 2011b). This implies that the occurrence of more intense TCs will cause an increase in wave set-up. Furthermore, water levels generally increase with decreasing water depth toward the shore (i.e., wave shoaling).

According to our results, the coastal area at Melekeok reef will be at greater risk of damage from large waves and increased water level by 2100. For example, TCs generating large waves typically cause significant beach erosion, as occurred in Tuvalu (Connell, 1999; Sato et al., 2010). Moreover, if storm surges occur, the coastal area at Melekeok reef will be flooded (Table 4). This could lead to the destruction of infrastructure, because many buildings (including the elementary school) are located at ~3 m above the MSL. In addition, saltwater intrusion into groundwater could cause long-term problems for water management, including declining water quality for drinking and agriculture (Rotzoll and Fletcher, 2013).

4.2 Coastal risk reduction through future reef growth

Our results indicate that there is no significant change in WL_s between a degraded reef and a healthy reef. This can be explained by the nature of coral reefs, which are porous structures characterized by a high degree of water permeability. A reef framework has a wide range of porosities from low (e.g., internal cavities have been infilled with marine cements) to high (e.g., a reef framework is mainly composed of branching corals) (Hopley, 2011). In this study, the mean porosity of reef framework is estimated as 10 %. This means that sea water permeates through the reef due to porosity, even if the reef is characterized by three dimensional structures. The above implies that a decreasing of SWH_r is very important to reduce the risks of costal damages. If SWH_r increases by only 0.1 m, it will lead to an increase in risks of substantial coastal damages such as flooding, destructions of constructions (houses and buildings), saltwater intrusion into groundwater, and coastal erosion, because the future WL_s will almost reach the elevation of the road at the study site. Detail quantity of the damages was beyond the scope of the present study, but flooding mostly occurs within a 1-km wide coastal zone along the shoreline, and a 0.33 m sea level rise has little effect on inundation, but a 0.66 m sea level rise, causes widespread groundwater inundation of the land surface at Oahu Island in Hawaii (Rotzoll and Fletcher, 2013), although it is difficult to directly compare a coastal area between the Melekeok reef and the results for Oahu Island.

In contrast to the results of WL_s, the healthier a reef, the greater its effectiveness at reducing SWH_r in the future. On average, reef growth resulted in an increase in the reduction rate from SWH_o to SWH_r of 84.6% to 86.0%, and it reduced SWH_r by a maximum of 0.44 m. The reduction is explained by the following three processes. (1) Future coral growth in the reef crest–upper reef slope zone will increase the dissipation of waves breaking as the water depth decreases (Figure 9). The breaking of waves will occur in shallow water when the ratio of wave height to water depth approaches 0.8 (Gourlay et al.,

2011c). Based on many field observations at other reefs and the results of water tank experiments (Takayama et al., 1977; Nakajima et al., 2011), a rapid decrease in water depth at the zone results in an increase in wave breaking. (2) Upward reef growth will increase the reef angle in the wave breaking zone as a result of a rapid decrease in water depth in this zone. This process also results in an increase in wave breaking. (3) With upward reef growth the wave breaking zone will probably migrate from its present location towards the ocean. This process will expand the area of wave height reduction, and consequently wave heights will decrease at the reef flat. Consequently, the above factors emphasize the need for future reef formation and growth to reduce the risk of damage by waves.

However, our results showed that only in 6 cases (cases 3, 6, 14, 17, 23, and 26) the SWH_r was increased to 0.02 m– 0.18 m by upward reef growth by 2100. One possible explanation of an increase in SWH_r is a difference in magnitude of infragravity waves between the degraded reef and the healthy reef. Infragravity waves over shallow reef flats are generated by relationships between the offshore conditions and reef flat characteristics (e.g., complex bathymetry). Waves propagating onto shallow reefs steepen and break, and while some of the breaking wave energy propagates shoreward as reformed high-frequency waves, the spectral wave energy shifts into lower frequencies and long-period (infragravity) waves often dominate (Cheriton et al., 2016). Increased wave height and water level due to the infragravity waves have been observed for various coral reefs (Nakaza et al., 1994; Cheriton et al., 2016) and have also been obtained in laboratory and modelling studies (Nakaza et al., 1994; Roeber and Bricker, 2015; Shimozono et al., 2015). Under normal wave conditions, the effect may be negligible in most cases. In contrast, in extreme wave conditions during tropical cyclones, extreme waves enhance the effect on coral reefs. For these 6 cases, the upward reef growth reduces water depth in the reef crest–upper reef slope zone and it probably enhances a resonant oscillation of water by infragravity waves. We compared a test case under normal wave conditions (2.0 m SWH_o, 9.0 s SWP_o) with case 23 under TC conditions (11.0 m SWH_o, 15.0 s SWP_o). The result showed that the SWH_r was decreased to 0.01 m by upward reef growth (unpublished data). But, the infragravity waves are known to be generated across the coral reef through nonlinear wave interactions and its overall effect remains unclear. Moreover, the occurrence of increase in SWH_r may be explained by an insufficient calculation time. We used a calculation data of 1800 s for the analysis of SWH_r. To better understand the difference in SWH_r between healthy reefs and degraded reef, a long calculation time will be probably needed. Additionally, reef coasts are often influenced by lateral flows such as diffracted waves due to topographic effects. In order to understand the complex behavior of waves, 3D-wave analysis using a 3D-wave model (e.g., Delft-3D: Deltares, 2017) will be required. Moreover, a water tank experiment would be required to investigate the effect of upward reef growth to the difference in SWH_r.

4.3 Reef production rate needed for coastal risk reduction

According to the analysis of drilled core in this study, a corymbose *Acropora* facies at a high-wave energy condition in water depths less than 7 m and an arborescent *Acropora* facies at a low- to moderate- wave conditions in water depths less than 20 m contributed to the Holocene reef growth in the Palau Islands (Kayanne et al., 2002; Hongo and Kayanne, 2011). The

maximum future SLR is predicted to be +0.98 m by 2100 (Church et al., 2013). This implies that arborescent *Acropora* corals will probably be overturned and broken by high wave energy in shallow water depths, and so will not contribute to upward reef formation at the reef crest by 2100. In contrast, corymbose corals at the study site will contribute to reef formation by 2100, in response to future SLR. Although the dominant corals at Melekeok reef have yet to be documented,

5   the corymbose *Acropora* facies on reef crests in the Palau Islands is generally composed of *A. digitifera*, *Acropora hyacinthus*, and *Acropora humilis* (Kayanne et al., 2002; Yukihira et al., 2007). These coral types are highly resistant to wave action at water depths of 0–7 m, and their preferred habitat (good light penetration and high oxygen concentrations) enables vigorous upward growth.

      Our results indicate that if the present MSL increases by 0.44 m (mean value for RCP 2.6) to 0.74 m (mean value

10   for RCP 8.5) by 2100, maintaining reductions in the wave height at the study reef will require 2.6–4.4 kg $CaCO_3/m^2/y$ to support upward reef growth by the corymbose *Acropora* facies (Figure 8d). Similarly, 5.8 kg $CaCO_3/m^2/y$ will be required to maintain wave height reduction by the facies under 0.98 m SLR by 2100 (highest value for RCP 8.5). Field measurements of the reef crest community at the core site following the mass bleaching event in 1998 showed that the calcification rate decreased from 130 to 74 mmol $C/m^2/day$, equivalent to a rate of 4.7–2.7 kg $CaCO_3/m^2/y$ (Kayanne et al., 2005). Coinciding

15   with the bleaching event, the coral cover decreased from 8.1% to 1.4% (Kayanne et al., 2005). Therefore, if the coral cover is ~1%, the corals will keep pace with 0.44 m SLR under RCP 2.6 by 2100, but >8% coral cover will be needed under RCP 8.5 to reduce wave height and the risk of coastal damage at the study site.

      However, if mortality of corymbose *Acropora* occurs at the study reef in the future because of global impacts (particularly elevated sea surface temperature and ocean acidification) and/or local stresses, it will probably cause a decline

20   in reef effectiveness in reducing wave height. Coral calcification is considered to be highly sensitive to elevated sea surface temperature and ocean acidification. Although there is variability in calcification rates among coral species (Pandolfi et al., 2011), corymbose *Acropora* species (e.g., *A. digitifera*) are particularly vulnerable to thermal stresses (Loya et al., 2001; Golbuu et al., 2007). The growth of *Acropora* at Okinawa Island in the Ryukyu Islands was significantly reduced by ocean acidification (Suwa et al., 2010). Local stresses, including sediment discharge, also have a negative impact on the species

25   (Burke et al., 2011; Hongo and Yamano, 2013). In Palau, there was a major decline in juvenile acroporidae corals at the reef slope on Melekeok and along the eastern reef slopes in Palau Islands after Typhoon Bopha in 2012 and Typhoon Haiyan in 2013 (Gouezo et al., 2015). Therefore, the loss of mature coral colonies on the eastern reef slopes after the typhoon may have decreased coral recruitments and led to the opening of space for turf algae (Gouezo et al., 2015). Our calculations for case 9 (TC: 8.70 m SWH_o, 13.0 s SWP_o; SLR 0.74 m) show that for a healthy reef, 0.74 m/kyr of upward growth produced a

30   reduction of 0.23 m in SWH_r in 2100. If the reef growth rate decreases to 3.7 m/kyr, a reduction of 0.05 m in SWH_r would be expected (unpublished data). Despite the decrease in juvenile acroporidae corals at Palau Islands, early successional corals, especially pocilloporidae, recruited 6 months after Typhoon Haiyan in 2013 (Gouezo et al., 2015). There is no information for upward reef growth by pocilloporidae in the islands. To understand the role in coastal risk reductions, an estimation of reef production by pocilloporidae will need to be considered.

4.4 Reduction of global disaster risk based on the health of coral reefs

This study highlights that the maintaining reef growth (as a function of coral cover) in the future is effective in reducing the risk of coastal damage arising from wave action. Therefore, further efforts for reef conservation are suggested to become more and more important. It is necessary to monitor the cover of reef-building corals, the recruitment of coral larvae, and the occurrence of various stressors. For example, the Palau Islands has a Protected Areas Network (PAN), which consists of marine and terrestrial areas established for the protection of important biological habitats. Enhancement of protected areas, appropriate management, and restoration efforts (e.g. coral transplantation) could be potential options to keep the health reef. Additionally, we recognize that the ground elevation of construction varies between each building. To efficiently evacuate the people from the flooding area, an investigation of ground elevation at each construction as well as the installation of signboard of elevation will be required. Furthermore, to evaluate the impact of hydrodynamic forces at coastal areas in the islands, establishment of *in situ* observation systems of wave height, wave period, and water level should be considered. For example, establishment of ultrasonic-wave-based wave gauges, observation buoys, and radar-based wave meters are recommended to predict accurately the ocean wave heights and periods to alert people of disasters such as flooding during TCs.

More than 150,000 km of shoreline in 100 countries and territories is thought to receive protection from reefs, which reduce wave energy (Burke et al., 2011). More than 100 million people in Southeast Asia live in reef-associated areas (i.e., within 10 km of the coast and within 30 km of a reef), where fringing reefs predominate (Burke et al., 2011). By 2100 this area and its people are likely to be at risk from wave action because of the increasing intensity of TCs, SLR, and storm surges, and this is likely to have negative economic and social effects. This study focused on Melekeok reef in the Palau Islands, but our results are applicable to other reefs in the Indo-Pacific and Caribbean regions. The natural breakwater formed by reefs is more cost-effective in coastal protection than the construction of artificial defences (Ferrario et al., 2014). Inexpensive but effective plans for coastal protection will be needed by small island nations and developing countries. Reef growth is self-adapting to long-term environmental change including SLR; it also provides a habitat for marine organisms and societal benefits including marine products, tourism, and recreation. Further research is needed to develop a policy of disaster risk reduction based on coral reef growth in the Indo-Pacific and Caribbean regions.

5 Conclusion

This study predicted the risk of coastal damage at Melekeok reef in the Palau Islands in the case of intensified TCs, SLR, and storm surges that are likely to occur during the 21st century. Our results, based on wave height and water level using the CADMAS-SURF wave simulation model, and past coral assemblage and reef growth rates estimated from the drilled core, indicate that the present-day reef is highly effective at dissipating incoming waves. However, more intense TCs, SLR, and storm surges resulting from climate change will increase wave height at the study site reef flat and water level at the shore.

This will increase the risk of beach erosion, saltwater intrusion into groundwater, and damage to infrastructure. Our sedimentological analysis suggests that reef formation by key reef-building corals, including corymbose *Acropora* (e.g., *A. digitifera*), may respond to future SLR. The upward reef growth will decrease the wave height on the reef flat, and reduce the risk of coastal damage. The use of coral reefs for disaster risk reduction is a cost-effective approach and includes other benefits derived from the various ecological services provided by living reefs. Future research such as that described in this study will be required for designing ecosystem-based disaster risk reduction policies for small island nations and for developing and developed countries alike.

Our research would be useful in predicting wave height and water level on coral reefs in the present climate and in a future climate. However, the research requires the following improvements. The present study emphasizes that further research is required regarding a short-term variation in sea level. During the El Niño of early 1998, mean sea level was ca. 0.20 m lower than normal in Palau Islands (Colin, 2009). This was quickly followed by the La Niña of late 1998, during this period the mean sea level was 0.35 m above normal (Colin, 2009). This was a half-meter change in mean sea level over just a few months. Such information will allow us to better understand changes in wave height and water level in the Palau Islands by 2100. Moreover, the CADMAS-SURF wave simulation model can contribute to our projecting of wave height and water level. Our study showed that there was a small differences in wave height and water level between *in situ* measurements and calculations on the reef flat under non-TCs conditions. To accurately validate for the model, further *in situ* measurements of wave height and water level under TCs conditions will be needed. The present study assumed a significant wave height and a significant wave period as a regular wave under TCs; however, coral reefs during TCs are affected by irregular waves. Consequently, it is necessary to set irregular waves for various TCs conditions using the CADMAS-SURF model and/or other 3D-wave model. Finally, the input parameters for the CADMAS-SURF model are obtained at 27 km resolution using the GFS model. To precisely estimate SWH_r and WL_s, *in situ* observed data of wave height, wave period, and water level should be collected.

Supplement

Table S1 Effects of intensification of tropical cyclones, and increased sea level rise and storm surges on wave height on the reef flat at the study site.

Table S2 Effects of intensification of tropical cyclones, and increased sea level rise and storm surges on water level at the shore at the study site.

Author contribution

C. Hongo had the idea and C. Hongo and H. Kurihara designed this research. All authors conducted data analysis, and the writing of the manuscript.

Competing interests

The authors declare that they have no conflict of interest.

Acknowledgements

The authors thank staff of the Palau International Coral Reef Center for help with field studies. This research was supported
by Japan Science and Technology (JST), the Japan International Cooperation Agency (JICA), and the Science and
Technology Research Partnership for Sustainable Development (SATREPS).

References

Anthony, K.R.N., Kline, D.I., Diaz-Pulido, G., Dove, S., and Hoegh-Guldberg, O.: Ocean acidification causes bleaching and
    productivity loss in coral reef builders, Proc. Natl. Acad. Sci. U.S.A., 105, 17442–17446, doi:10.1073/pnas.0804478105,
    2008.

Benedict, M.A. and McMahon, E.T.: Green infrastructure: smart conservation for the 21st century, Sprawl Watch
    Clearinghouse, Washington, D.C., 2002.

Burke, L., Reytar, K., Spalding, M., and Perry, A.: Reefs at Risk Revisited, World Resources Institute, Washington, D.C.,
    2011.

Chappell, J. and Polach, H.: Post glacial sea level rise from a coral record at Huon Peninsula, Papua New Guinea, Nature,
    349, 147–149, doi:10.1038/349147a0, 1991.

Cheriton, O.M., Storlazzi, C.D., and Rosenberger, K.J.: Observations of wave transformation over a fringing coral reef and
    the importance of low-frequency waves and offshore water levels to runup, overwash, and coastal flooding, J. Geophys.
    Res., 121, 3121–3140, doi: 10.1002/2015JC011231, 2016.

Christensen, J.H., Krishna Kumar, K., Aldrian, E., An, S.-I., Cavalcanti, I.F.A., de Castro, M., Dong, W., Goswami, P., Hall,
    A., Kanyanga, J.K., Kitoh, A., Kossin, J., Lau, N.-C., Renwick, J., Stephenson, D.B., Xie, S.-P., and Zhou,T.: Climate
    phenomena and their relevance for future regional climate change, In: Stocker, T.F., Qin, D., Plattner, G.-K., Tignor, M.,
    Allen, S.K., Boschung, J., Nauels, A., Xia, Y., Bex, V., and Midgley, P.M. (Eds) Climate change 2013: The Physical
    Science Basis, Cambridge University Press, Cambridge and New York, pp. 1217–1308, 2013

Church, J.A., Clark, P.U., Cazenave, A., Gregory, J.M., Jevrejeva, S., Levermann, A., Merrifield, M.A., Milne, G.A., Nerem,
    R.S., Nunn, P.D., Payne, A.J., Pfeffer, W.T., Stammer, D., and Unnikrishnan, A.S.: Sea level change, In: Stocker, T.F.,
    Qin, D., Plattner, G.-K., Tignor, M., Allen, S.K., Boschung, J., Nauels, A., Xia, Y., Bex, V., and Midgley, P.M. (Eds)
    Climate change 2013: The Physical Science Basis, Cambridge University Press, Cambridge and New York, pp. 1137–
    1216, 2013

Coastal Development Institute of Technology (CDIT): Research and Development of Numerical Wave Flume: CADMAS-SURF, Coastal Development Institute of Technology, Tokyo, 2001.

Colin, P.L.: Marine Environments of Palau, Mutual Publishing LLC, Honolulu, 2009.

Connell, J.: Environmental change, economic development, and emigration in Tuvalu, Pacific Studies, 22, 1–20, 1999.

5   Deltares: Delft3D-FLOW User manual: Simulation of multi-dimensional hydrodynamic flows and transport phenomena, including sediments. Version 3.15, Deltares, Delft, 2017.

Ferrario, F., Beck, M.B., Storlazzi, C.D., Micheli, F., Sheppard, C.C., and Airoldi, L.: The effectiveness of coral reefs for coastal hazard risk reduction and adaptation, Nat. Commun., 5, 3794, doi:10.1038/ncomms4794, 2014.

Frank, W.M. and Young, G.S.: The Interannual Variability of Tropical Cyclones, Mon. Weather Rev., 135, 3587–3598,
10   doi:http://dx.doi.org/10.1175/MWR3435.1, 2007.

Global Facility for Disaster Reduction and Recovery (GFDRR): GFDRR annual report 2015: Bringing resilience to scale. Global Facility for Disaster Reduction and Recovery, Washington, D.C., 2016.

Golbuu, Y., Fabricius, K., and Okaji, K.: Status of Palau's coral reefs in 2005, and their recovery from the 1998 bleaching event, In: Kayanne, H., Omori, M., Fabricius, K., Verheij, E., Colin, P., Golbuu, Y., Yukihira, H. (Eds.) Coral Reefs of
15   Palau. Palau International Coral Reef Center, Palau, pp. 40–50, 2007.

Gouezo, M., Golbuu, Y., van Woesik, R., Rehm, L., Koshiba, S., and Doropoulos, C.: Impact on two sequential super typhoons on coral reef communities in Palau, Mar. Ecol.-Prog. Ser., 540, 73–85, doi:https://doi.org/10.3354/meps11518, 2015.

Gourlay, M.R.: Infrastructure and reef islands, In: Hopley, D. (Ed.), Encyclopedia of Modern Coral Reefs. Springer,
20   Dordrecht, pp. 601–607, 2011a.

Gourlay, M.R.: Wave set-up, In: Hopley, D. (Ed.), Encyclopedia of Modern Coral Reefs. Springer, Dordrecht, pp. 1144–1149, 2011b.

Gourlay, M.R.: Wave shoaling and refraction, In: Hopley, D. (Ed.), Encyclopedia of Modern Coral Reefs. Springer, Dordrecht, pp. 1149–1154, 2011c.

25   Hongo, C., Kawamata, H., and Goto, K.: Catastrophic impact of typhoon waves on coral communities in the Ryukyu Islands under global warming, J. Geophys. Res., 117, G02029, doi:10.1029/2011JG001902, 2012.

Hongo, C. and Kayanne, H.: Holocene sea-level record from corals: Reliability of paleodepth indicators at Ishigaki Island, Ryukyu Islands, Japan, Paleogeogr. Paleoclimatol. Paleoecol., 287, 143–151, doi:10.1016/j.palaeo.2010.01.033, 2010.

Hongo, C. and Kayanne, H.: Key species of hermatypic coral for reef formation in the northwest Pacific during Holocene
30   sea-level change, Mar. Geol., 279, 162–177, doi:10.1016/j.margeo.2010.10.023, 2011.

Hongo, C. and Yamano, H.: Species-specific responses of corals to bleaching events on anthropogenically turbid reefs on Okinawa Island, PLOS ONE 8, e60952, doi:10.1371/journal.pone.0060952, 2013.

Hopley, D.: Density and porosity: influence on reef accretion rates, In: Hopley, D. (Ed.), Encyclopedia of Modern Coral Reefs. Springer, Dordrecht, pp. 303–304, 2011.

IPCC, 2013: Annex III: Glossary [Planton S. (Ed)], In: Stocker, T.F., Qin, D., Plattner, G.-K., Tignor, M., Allen, S.K., Boschung, J., Nauels, A., Xia, Y., Bex, V., and Midgley, P.M. (Eds) Climate change 2013: The Physical Science Basis, Cambridge University Press, Cambridge and New York, pp. 1447–1465, 2013.

Isobe, M., Takahashi, S., Yu, S.P., Sakakiyama, T., Fujima, K., Kawasaki, K., Jiang, Q., Akiyama, M., and Ohyama, H.: Interim development of a numerical wave flume for maritime structure design, Proceedings of Civil Engineering in the Ocean 15, 321–236, 1999.

Japan Meteorological Agency (JMA): Annual Report of Ocean wave in 2005. CD-ROM, 2012.

Kawasaki, K., Kiku, M., Maezato, K., Komesu, T., Shimada, H., Gomi, H., Shibata, T., and Itabashi, N.: Examination of countermeasures against wave overtopping around revetment using numerical wave flume, Proceedings of Coastal Engineering, Japan Society of Civil Engineers, 54, 951–955, 2007.

Kawasaki, K., Kiku, M., Sasada, Y., Maezato, K., Uchima, Y., Shimada, H., Gomi, H., Miura, K., and Shibata, T.: Effects of bottom topography and revetment configuration on wave overtopping characteristics of coastal revetment in regular/ irregular wave field, Proceedings of Coastal Engineering, Japan Society of Civil Engineers, 55, 831–835, 2008.

Kayanne, H., Yamano, H., and Randall, R.H.: Holocene sea-level changes and barrier reef formation on an oceanic island, Palau Islands, western Pacific, Sediment. Geol., 150, 47–60, doi:10.1016/S0037-0738(01)00267-6, 2002.

Kayanne, H., Hata, H., Kudo, S., Yamano, H., Watanabe, A., Ikeda, Y., Nozaki, K, Kato, K, Negishi, A., and Saito, H.: Seasonal and bleaching‐induced changes in coral reef metabolism and CO_2 flux, Glob. Biogeochem. Cycle, 19, GB3015, doi:10.1029/2004GB002400, 2005.

Loya, Y., Sakai, K., Yamazato, K., Nakano, Y., Sambali, H., and Van Woesik, R.: Coral bleaching: the winners and the losers, Ecol. Lett., 4, 122–131, doi:10.1046/j.1461-0248.2001.00203.x, 2001.

Maragos, J.E., and Cook C.W.: The 1991–1992 rapid ecological assessment of Palau's coral reefs, Coral Reefs, 14, 237–252, doi: 10.1007/BF00334348, 1995.

Montaggioni, L.F.: History of Indo-Pacific coral reef systems since the last glaciation: Development patterns and controlling factors, Earth-Sci. Rev., 71, 1–75, doi:10.1016/j.earscirev.2005.01.002, 2005.

Montaggioni, L.F. and Braithwaite, C.J.R.: Quaternary coral reef systems: History, development, process and controlling factors. Elsevier, Amsterdam, 2009.

Murakami, H., Wang, B., and Kitoh, A.: Future change of western North Pacific typhoons: projections by a 20-km-mesh global atmospheric model. J. Climate, 24, 1154–1169, doi: 10.1175/2010JCLI3723.1, 2011.

Nagai, H., and Shiraishi, S.: Study on stability of immersed tunnel against waves, Report of the Coastal Development Institute of Technology, 4, 41–44, 2004.

Nakajima, S., Sekimoto, T., Katayama, H., and Takahashi, K.: Experimental study on wave transformation on steep coral reef, Journal of Japan Society of Civil Engineers B3, 67, I_244–I_249, 2011.

Nakamura, M., Arashiro, Y., and Shiga, S.: Numerical simulations to account for boulder movements on Lanyu Island, Taiwan: tsunami or storm?, Earth, Planets and Space, 66,128, doi:10.1186/1880-5981-66-128, 2014.

Nakaza, E., Tsukayama, S., and Tanaka, S.: Waves and surf beats induced by wave group on coral reef flat, Proceedings of Coastal Engineering, Japan Society of Civil Engineers 41, 86–90, 1994.

Pandolfi, J.M., Connolly, S.R., Marshall, D.J., and Cohen, A.L.: Projecting coral reef futures under global warming and ocean acidification, Science, 333, 418–422, doi:10.1126/science.1204794, 2011.

5   Rechebei, E.D. and McPhetres, S.F.: History of Palau: Heritage of an emerging nation. The Ministry of Education, Republic of Palau, Koror, 1997.

Roeber, V. and Bricker, J.D.: Destructive tsunami-like wave generated by surf beat over a coral reef during Typhoon Haiyan, Nat. Commun., 6, 7854, doi:10.1038/ncomms8854, 2015.

Rotzoll, K. and Fletcher, C.H.: Assessment of groundwater inundation as a consequence of sea-level rise, Nat. Clim. Chang., 10   3, 477–481, doi:10.1038/nclimate1725, 2013.

Sato, D., Yokoki, H., Sakurai, M., and Kuwahara, Y.: Lagoonal wave field on tropical cyclone condition in Funafuti atoll, Tuvalu, Journal of Japan Society of Civil Engineers B2, 66, 1236–1240, 2010.

Seneviratne, S.I., Nicholls, N., Easterling, D., Goodess, C.M., Kanae, S., Kossin, J., Luo, Y., Marengo, J., McInnes, K., Rahimi, M., Reichstein, M., Sorteberg, A., Vera, C., and Zhang, X.: Changes in climate extremes and their impacts on the 15   natural physical environment, In: Field, C.B., Barros, V., Stocker, T.F., Qin, D., Dokken, D.J., Ebi, K.L., Mastrandrea, M.D., Mach, K.J., Plattner, G.-K., Allen, S.K., Tignor, M., and Midgley, P.M. (Eds.) Managing the Risks of Extreme Events and Disasters to Advance Climate Change Adaptation. A Special Report of Working Groups I and II of the Intergovernmental Panel on Climate Change (IPCC). Cambridge University Press, Cambridge and New York, pp. 109–230, 2012.

20   Sheppard, C., Dixon, D. J., Gourlay, M., Sheppard, A., and Payet, R.: Coral mortality increases wave energy reaching shores protected by reef flats: examples from the Seychelles, Estuar. Coast. Shelf Sci., 64, 223–234, doi:10.1016/j.ecss.2005.02.016, 2005.

Shimozono, T., Tajima, T., Kennedy, A.B., Nobuoka, H., Sasaki, J., and Sato, S.: Combined infragravity wave and sea swell runup over fringing reefs by super typhoon Haiyan, J. Geophys. Res., 120, doi:10.1002/2015JC010760, 2015.

25   Suwa, R., Nakamura, M., Morita, M., Shimada, K., Iguchi, A., Sakai, K., and Suzuki, A.: Effects of acidified seawater on early life stages of scleractinian corals (Genus *Acropora*), Fish. Sci., 76, 93–99, doi:10.1007/s12562-009-0189-7, 2010.

Takayama, T., Kamiyama, Y., and Kikuchi, O.: Wave transformation on a reef, In: The Port and Harbour Research Institute, Ministry of Transport, Japan (Ed.) Technical note of the Port and Harbour Research Institute, Ministry of Transport, Japan. The Port and Harbour Research Institute, Ministry of Transport, 278, Yokosuka, pp. 1–32, 1977.

30   Tsuboki, K, Yoshioka, M.K., Shinoda, T, Kato, M., Kanada,S., and Kitoh, A.: Future increase of supertyphoon intensity associated with climate change, Geophys. Res. Lett., 42, 646–652, doi:10.1002/2014GL061793, 2015.

United States Geological Survey (USGS): Topographic map of Oreor, Republic of Palau, Caroline Islands. USGS, Denver, 1983.

Watanabe, M., Goto, K., Imamura, F., and Hongo, C.: Numerical identification of tsunami boulders and estimation of local tsunami size at Ibaruma reef of Ishigaki Island, Japan, Island Arc 25, 316–332, doi:10.1111/iar.12115, 2016.

Wong, P.P., Losada, I.J., Gattuso, J.-P., Hinkel, J., Khattabi, A., McInnes, K.L., Saito, Y., and Sallenger, A.: Coastal systems and low-lying areas, In: Field, C.B., Barros, V.R., Dokken, D.J. Mach, K.J., Mastrandrea, M.D., Bilir, T.E., Chatterjee, M., Ebi, K.L., Estrada, Y.O., Genova, R.C., Girma, B., Kissel, E.S., Levy, A.N., MacCracken, S., Mastrandrea, P.R., and White, L.L. (Eds.) Climate Change 2014: Impacts, Adaptation, and Vulnerability. Part A: Global and Sectoral Aspects. Contribution of Working Group II to the Fifth Assessment Report of the Intergovernmental Panel on Climate Chang, Cambridge University Press, Cambridge and New York, pp. 361–409, 2014.

Woodruffe, J.D., Irish, J.L., and Camargo, S.J.: Coastal flooding by tropical cyclones and sea-level rise, Nature, 504, 44–52, doi:10.1038/nature12855, 2013.

The World Bank, The United Nations (UN): Natural hazard, unnatural disasters: the economics of effective prevention, The World Bank, Washington, D.C. , 2010.

Yamashita, T., Nakamura, Y., Miyagi, E., Oka, H., Nishioka, Y., Takeuchi, H., Kyan, T., and Hoshi, M.: Evaluation of inundation and damage caused by tsunamis and storm surges on the coast of Okinawa Prefecture, Proceedings of Coastal Engineering, Japan Society of Civil Engineers, 55, 306–310, 2008.

Yokoyama, Y., Nakada, M., Maeda, Y., Nagaoka, S., Okuno, J., Matsumoto, E., Sato, H., and Matsushima, Y.: Holocene sea-level change and hydro-isostasy along the west coast of Kyusyu, Japan, Paleogeogr. Paleoclimatol. Paleoecol., 123, 29–47, doi:10.1016/0031-0182(95)00112-3, 1996.

Yokoyama, Y., Maeda, Y., Okuno, J., Miyairi, Y., and Kosuge, T.: Holocene Antarctic melting and lithospheric uplift history of the southern Okinawa trough inferred from mid- to late-Holocene sea level in Iriomote Island, Ryukyu, Japan, Quat. Int., 397, 342–348, doi:10.1016/j.quaint.2015.03.030, 2016.

Yukihira, H., Shimoike, K., Golbuu, Y., Kimura, T., Victor, S., and Ohba, H.: Coral reef communities and other marine biotopes in Palau, In: Kayanne, H., Omori, M., Fabricius, K., Verheij, E., Colin, P., Golbuu, Y., Yukihira, H. (Eds.) Coral Reefs of Palau. Palau International Coral Reef Center, Palau, pp. 10–29, 2007.
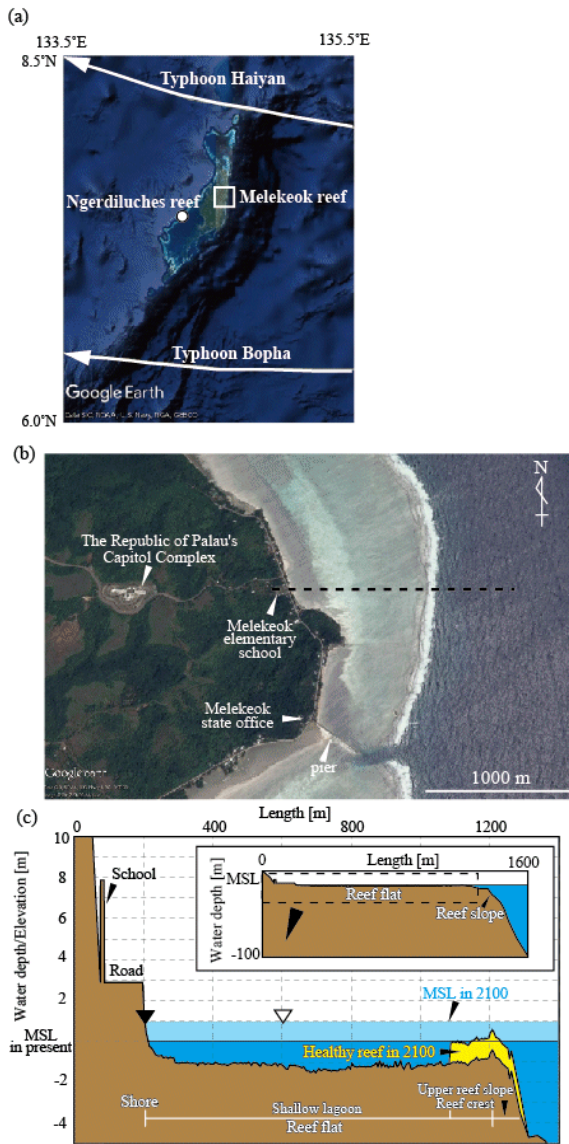
Figure 1: Location of Melekeok reef in the Palau Islands, and the reef topography used for wave calculations. (a) Location of Melekeok reef. The open circle indicates the drillcore site on Ngerdiluches reef (Kayanne et al., 2002). Typhoon Bopha passed south of Palau Islands on 2 December 2012 and Typhoon Haiyan passed north of the islands on 6–7 November 2013, provided by Digital Typhoon (http://agora.ex.nii.ac.jp/digital-typhoon/index.html.en). (b) Satellite image of the reefs, long beaches, the Republic of Palau's Capitol Complex, Melekeok elementary school, and Melekeok state office. The dashed line shows the location of the survey transect. (c) The measured cross-section, showing the present day and the 2100 reef topography. The reef crest and upper reef slope will be characterized by upward reef growth or cessation of growth in response to sea level rise (SLR). This figure shows the example of upward reef growth for a healthy reef in response to +0.98 m SLR in 2100, based on the Representative Concentration Pathway (RCP) 8.5 scenario (Church et al.,

2013). The open and solid triangles indicate the locations used for calculating the significant wave height at the reef flat (SWH$_r$) (400 m from the shore) and the water level at the shore (WL$_s$), respectively. MSL indicates mean sea level.
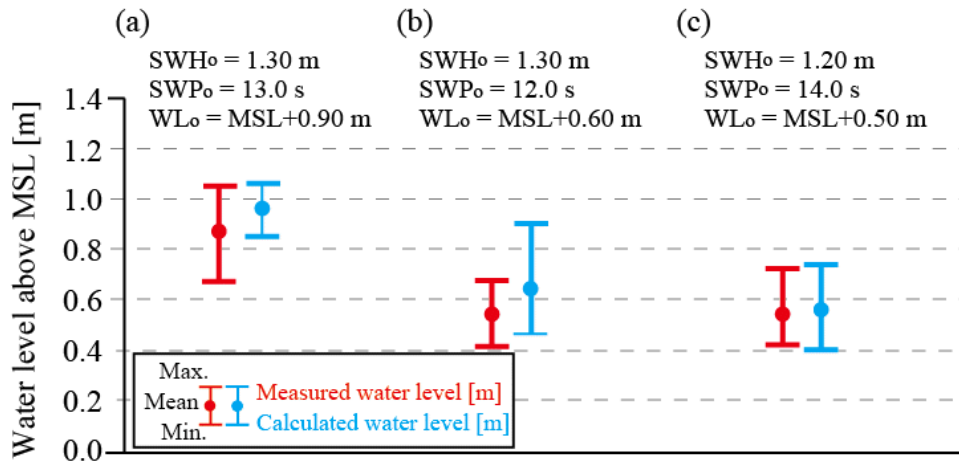
5   **Figure 2**: Comparison of *in situ* measurements and calculated results of water levels on the reef flat (400 m from the shore) at the study site. (a) Test1: The assumed SWH$_o$ and SWP$_o$ values were 1.30 m and 13.0 s, respectively. The assumed WL$_o$ value was +0.90 m above MSL. (b) Test 2: The assumed SWH$_o$ and SWP$_o$ values were 1.30 m and 12.0 s, respectively. The assumed WL$_o$ value was +0.60 m above MSL. (c) Test 3: The assumed SWH$_o$ and SWP$_o$ values were 1.20 m and 13.0 s, respectively. The assumed WL$_o$ value was +0.50 m above MSL.

Figure 3: Photograph of the coast at the study site. (a) A pavilion located in the coast. The elevation of the pavilion is less than 3 m above present MSL. (b) Damage of the foundation of pavilion due to the erosion during Typhoon Bopha. (c) Many cracks of the floor of the pavilion. (d) Photograph of the collapsed pier at Melekeok reef. (e) Photograph of the road and Melekeok elementary school along the coast. The elevation of the road is +2.86 m above present MSL. (f) Photograph of the ground of the school. The elevation of the ground is ca. 3 m above present MSL. The road and the ground were flooded during Typhoon Bopha.
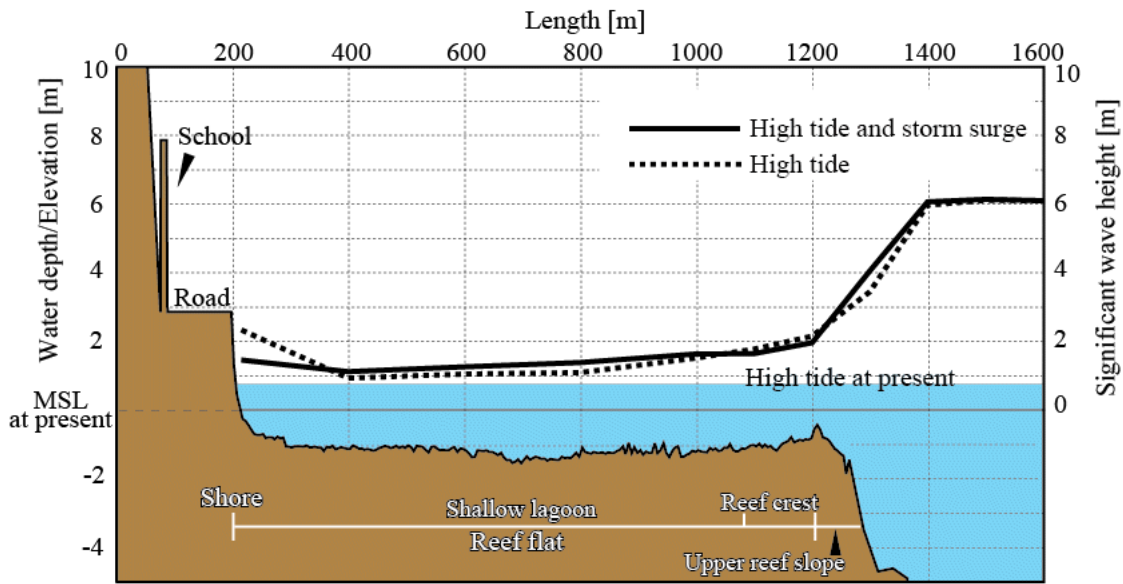
Figure 4: Calculated significant wave height (SWH) at the study site under high tide and storm surge (solid line) and high tide (dotted line). The assumed SWH_o and SWP_o values were 8.70 m and 13.0 s, respectively, for the present conditions model TC (i.e., Typhoon Bopha). The assumed WL_o was +0.80 m (i.e., high tide) and +1.80 m (i.e., high tide and storm surge) above the present MSL. Rapid wave breaking occurs in the upper reef slope–reef crest zone, whereas the reef flat is characterized by relatively calm conditions. The SWH value at the shore increases as the water depth decreases.
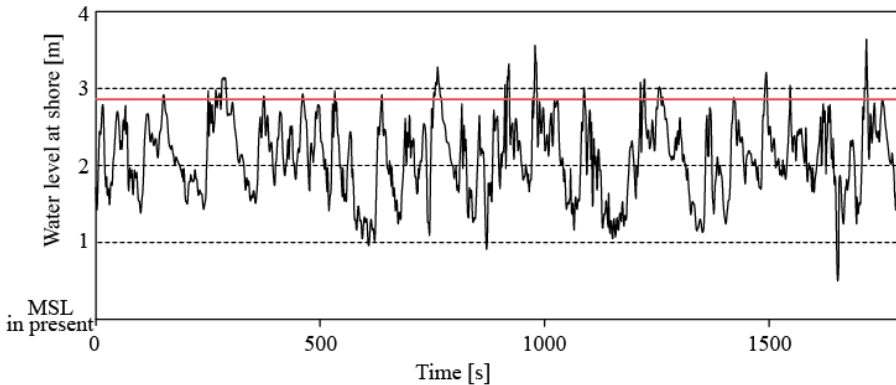
Figure 5: Calculated water level on the shore at the study site under the present-day TC (i.e., Typhoon Bopha). The assumed SWH_o and SWP_o values were 8.70 m and 13.0 s, respectively. The assumed WL_o was +1.80m above MSL (i.e., high tide and storm surge). The horizontal solid line in red shows the elevation of the road (+2.86 m above present MSL) at the study site. The road was frequently flooded.
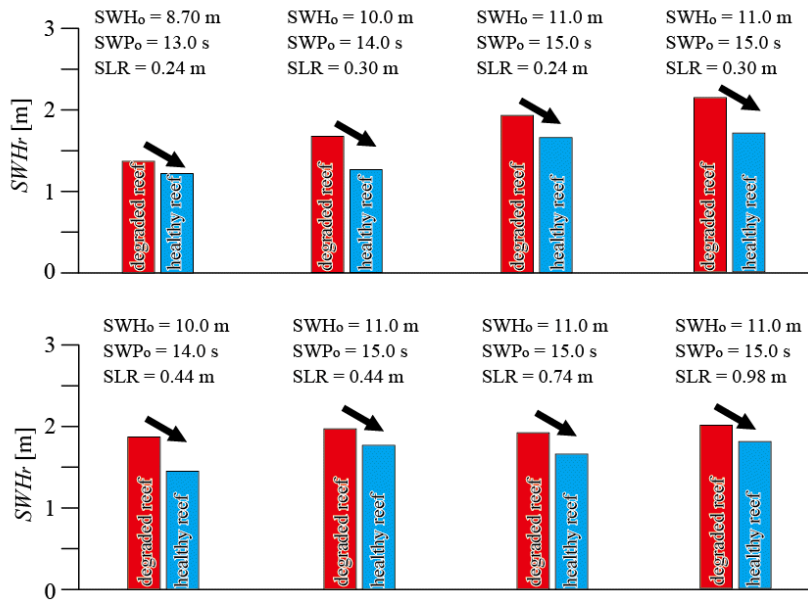
Figure 6: Effect of reef growth on change in the significant wave height at the reef flat for the TCs by 2100. Assumptions: 8.70–11.0 m SWH_o; 13.0–15.0 s SWP_o; SLR 0.24–0.98 m; 1.8 m above present MSL WL_o (i.e., high tide and storm surge). The SLR values are based on the values for the RCP scenario in 2100 (Church et al., 2013). The examples show that healthy reefs will reduce wave height.
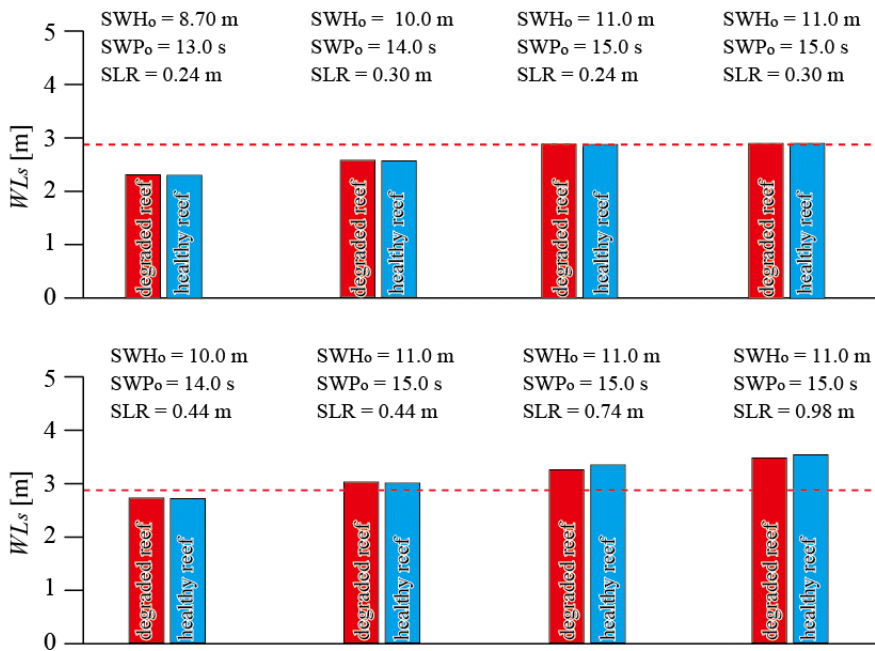
Figure 7: Effect of reef growth on change in the water level at the shore for the TCs by 2100. Assumptions: 8.70–11.0 m SWH_o; 13.0–15.0 s SWP_o; SLR 0.24–0.98 m; 1.8 m above present MSL WL_o (i.e., high tide and storm surge). The SLR values are based on the values

for the RCP scenario in 2100 (Church et al., 2013). The horizontal dashed line shows the elevation of the road (+2.86 m above present MSL) at the study site. The road will be frequently flooded even if the reef is healthy.

Rate of Holocene SLR	Rate of reef prodcution (kg CaCO₃/m²/y)		Rate of future SLR	Rate of potential reef prodcution (kg CaCO₃/m²/y)	
	arborescent *Acropora* facies	corymbose *Acropora* facies		arborescent *Acropora* facies	corymbose *Acropora* facies
10 m/kyr	(A) 2.4–26.7	(B) 14.2	9.8 m/kyr	(E) 7.1	(F) 5.8
5 m/kyr	—	(C) 1.3	7.4 m/kyr	(G) 5.3	(H) 4.4
<1 m/kyr	—	(D) 0.3	4.4 m/kyr	—	(I) 2.6
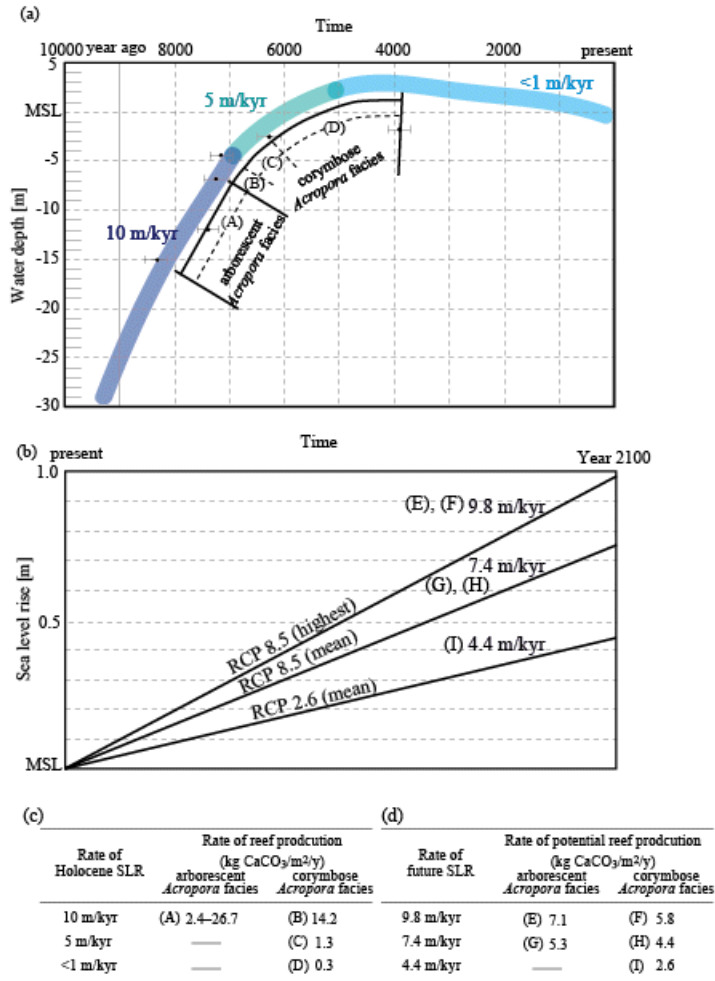
Figure 8: Past and future reef production rates at the study site. (a) Sedimentary facies and Holocene sea level curve relative to present MSL at the study site. Solid circles represent ¹⁴C ages obtained from the reef crest drillcore (PL-I: Kayanne et al., 2002). Radiometric counter errors are given in terms of two standard deviations (2σ). The reef growth curve is from Kayanne et al. (2002). The thick line shows two facies (arborescent *Acropora* facies and corymbose *Acropora* facies), from Hongo and Kayanne (2011). The dashed lines (A–D) indicate the period for estimation of the reef production rate for each facies in response to Holocene sea level change. The sea level curve around the study site is from Chappell and Polach (1991), Yokoyama et al. (1996, 2016), and Hongo and Kayanne (2010). (b) Sea level curve projected for 2100. The SLR ranges from +0.44 to +0.98 m until the end of the 21st century (RCP 2.6 and 8.5 scenarios; Church et al., 2013), equivalent to a SLR rate of 4.4–9.8 m/kyr. (E)–(I) Locations used for estimating reef production rates for each facies in response to future sea level change. (c) Holocene reef production rate based on drillcore. (D) Future potential reef production rate for each facies if the reef remains healthy.
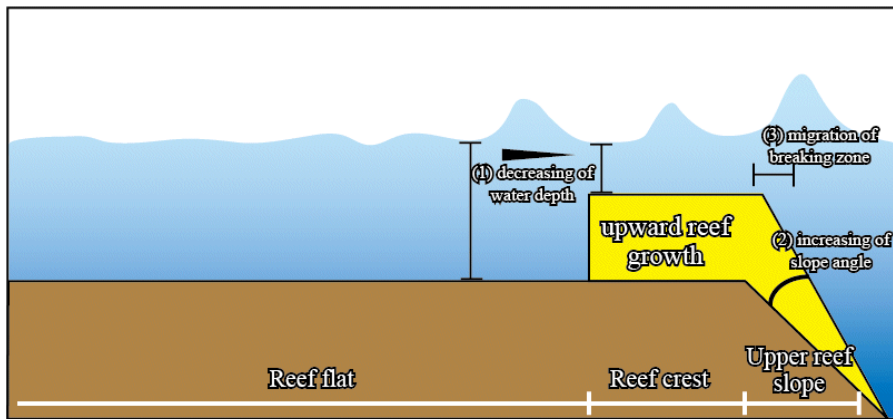
Figure 9: Effects of reef growth on reduction in wave height at the reef flat. In the reef crest to upper reef slope zone, upward reef growth will cause: (1) a decrease in water depth; (2) an increase in the reef slope angle; and (3) migration of the wave breaking zone towards the outer ocean. These processes will enhance wave breaking in the reef crest to upper reef slope zone relative to degraded reef. Consequently, wave height on the reef flat will be reduced.

Table 1 Tropical cyclone passing within 150 km of Melekeok reef from 1951 to 2015.

TC name	Approaching date	Minimum pressure of center (hPa)[a]	Nearest distance from Melekeok reef (km)[a]	Maximum wind speed at nearest distance from Melekeok reef (m/s)[a]
VIOLET	2 January 1955	995	81	NA
NO-NAME	4 January 1957	995	93	NA
SHIRLEY	11 April 1957	975	76	NA
RUBY	28 February 1959	998	127	NA
SALLY	11 March 1959	990	101	NA
GILDA	15 December 1959	925	121	NA
LOUISE	16 November 1964	915	105	NA
SALLY	3 March 1967	980	51	NA
SUSAN	20 April 1969	940	22	NA
THERESE	2 December 1972	945	32	NA
LOLA	22 January 1975	975	21	NA
MARIE	7 April 1976	930	99	NA
CECIL	13 April 1979	965	9	23
MAMIE	18 March 1982	990	71	23
JUDY	2 February 1986	970	139	20
MIKE	10 November 1990	915	44	45–50
SHARON	11 March 1991	985	66	25
BOPHA	2 December 2012	930	121	50
HAIYAN	7 November 2013	895	72	55–60

NA: Not available

[a] Estimated by Digital Typhoon (http://agora.ex.nii.ac.jp/digital-typhoon/) and based on Japan Meteorological Agency best track data.

Table 2 *In situ* Measurements and calculation conditions of water level and wave height for validation.

Case	In situ measurement				Calculation			
	Distance from shore (m)	Depth (m)	Tide (m above present mean sea level	Measured time (s)	SWH_o (m)	SWP_o (s)	WL_o (m)	Calculation time (s)
Test 1	400	0.62	0.90	1800	1.30	13.0	0.90	1800
Test 2	400	0.62	0.60	1800	1.30	12.0	0.60	1800
Test 3	400	0.62	0.50	1800	1.20	14.0	0.50	1800

SWH_o: significant wave height at outer ocean

SWP_o: significant wave period at outer ocean

WL_o : water level at the outer ocean (above present mean sea level)

Table 3: Significant wave heights at the study site.

Case	Year	SWH_o (m)	SWP_o (s)	SLR (m)	SWH_r at degraded reef (m)	Percent reduction of wave height from SWH_o to SWH_r at degraded reef	SWH_r at healthy reef (m)	Percent reduction of wave height from SWH_o to SWH_r at healthy reef
Without storm surge								
1	Present	8.70	13.0	0.00	-	-	1.05	87.9%
2	Year 2050	8.70	13.0	0.24	1.11	87.2%	0.88	89.9%
3	Year 2050	8.70	13.0	0.30	0.97	88.9%	1.09	87.5%
4	Year 2050	10.0	14.0	0.24	1.45	85.5%	1.21	87.9%
5	Year 2050	10.0	14.0	0.30	1.51	84.9%	1.46	85.4%
6	Year 2050	11.0	15.0	0.24	1.31	88.1%	1.49	86.5%
7	Year 2050	11.0	15.0	0.30	1.53	86.1%	1.50	86.4%
8	Year 2100	8.70	13.0	0.44	1.07	87.7%	1.06	87.8%
9	Year 2100	8.70	13.0	0.74	1.34	84.6%	1.11	87.2%
10	Year 2100	8.70	13.0	0.98	1.28	85.3%	1.12	87.1%
11	Year 2100	10.0	14.0	0.44	1.54	84.6%	1.33	86.7%
12	Year 2100	10.0	14.0	0.74	1.48	85.2%	1.18	88.2%
13	Year 2100	11.0	15.0	0.44	1.63	85.2%	1.40	87.3%
14	Year 2100	11.0	15.0	0.74	1.68	84.7%	1.77	83.9%
With storm surge of 1.00 m								
15	Present	8.70	13.0	0.00	-	-	1.24	85.7%
16	Year 2050	8.70	13.0	0.24	1.37	84.3%	1.22	86.0%
17	Year 2050	8.70	13.0	0.30	1.33	84.7%	1.35	84.5%
18	Year 2050	10.0	14.0	0.24	1.57	84.3%	1.52	84.8%
19	Year 2050	10.0	14.0	0.30	1.67	83.3%	1.26	87.4%
20	Year 2050	11.0	15.0	0.24	1.93	82.5%	1.66	84.9%
21	Year 2050	11.0	15.0	0.30	2.14	80.5%	1.70	84.5%
22	Year 2100	8.70	13.0	0.44	1.32	84.8%	1.21	86.1%
23	Year 2100	8.70	13.0	0.74	1.24	85.7%	1.40	83.9%
24	Year 2100	8.70	13.0	0.98	1.47	83.1%	1.30	85.1%
25	Year 2100	10.0	14.0	0.44	1.87	81.3%	1.45	85.5%
26	Year 2100	10.0	14.0	0.74	1.59	84.1%	1.64	83.6%
27	Year 2100	11.0	15.0	0.44	1.97	82.1%	1.77	83.9%
28	Year 2100	11.0	15.0	0.74	1.92	82.5%	1.66	84.9%
29	Year 2100	11.0	15.0	0.98	2.00	81.8%	1.80	83.6%

SWH_o: significant wave height at outer ocean

SWP_o: significant wave period at outer ocean

SLR: sea level rise, based on RCP scenarios 2.6 and 8.5 (Church et al., 2013).

SWH_r: significant wave height at reef flat

The tide is 0.80 m above present mean sea level (i.e., high tide).

Table 4: Flooding risk at the study site.

Case	Year	SWH$_o$ (m)	SWP$_o$ (s)	SLR (m)	WL$_s$ at degraded reef (m)	WL$_s$ at healthy reef (m)	Change in WL$_s$ from degraded reef to healthy reef (m)
Without storm surge							
30	Present	8.70	13.0	0.00	-	0.86	
31	Year 2050	8.70	13.0	0.24	1.19	1.24	-0.05
32	Year 2050	8.70	13.0	0.30	1.30	1.41	-0.11
33	Year 2050	10.0	14.0	0.24	1.58	1.55	0.03
34	Year 2050	10.0	14.0	0.30	1.54	1.64	-0.10
35	Year 2050	11.0	15.0	0.24	1.87	1.90	-0.03
36	Year 2050	11.0	15.0	0.30	1.97	1.99	-0.02
37	Year 2100	8.70	13.0	0.44	1.50	1.52	-0.02
38	Year 2100	8.70	13.0	0.74	1.82	1.90	-0.08
39	Year 2100	8.70	13.0	0.98	2.06	2.12	-0.06
40	Year 2100	10.0	14.0	0.44	1.82	1.81	0.01
41	Year 2100	10.0	14.0	0.74	2.09	2.07	0.02
42	Year 2100	11.0	15.0	0.44	2.07	2.12	-0.05
43	Year 2100	11.0	15.0	0.74	2.41	2.45	-0.04
With storm surge of 1.00 m							
44	Present	8.70	13.0	0.00	-	2.10	
45	Year 2050	8.70	13.0	0.24	2.30	2.29	0.01
46	Year 2050	8.70	13.0	0.30	2.42	2.35	0.07
47	Year 2050	10.0	14.0	0.24	2.44	2.53	-0.09
48	Year 2050	10.0	14.0	0.30	2.55	2.54	0.01
49	Year 2050	11.0	15.0	0.24	_2.87_	_2.86_	0.01
50	Year 2050	11.0	15.0	0.30	_2.89_	_2.89_	0.00
51	Year 2100	8.70	13.0	0.44	2.49	2.50	-0.01
52	Year 2100	8.70	13.0	0.74	2.81	2.83	-0.02
53	Year 2100	8.70	13.0	0.98	_3.00_	_3.01_	-0.01
54	Year 2100	10.0	14.0	0.44	2.70	2.69	0.01
55	Year 2100	10.0	14.0	0.74	_2.97_	_2.96_	0.01
56	Year 2100	11.0	15.0	0.44	_3.00_	_2.98_	0.02
57	Year 2100	11.0	15.0	0.74	_3.23_	_3.32_	-0.09
58	Year 2100	11.0	15.0	0.98	_3.45_	_3.51_	-0.06

SWH$_o$: significant wave height at outer ocean

SWP$_o$: significant wave period at outer ocean

SLR: sea level rise, based on RCP scenarios 2.6 and 8.5 (Church et al., 2013).

WL$_s$: water level at shore

Under line: over of risk level of flooding (2.86 m above present mean sea level)

The tide is 0.80 m above present mean sea level (i.e., high tide).